

REDUCED-ORDER MODEL FOR LARGE AMPLITUDE VIBRATIONS OF FLEXIBLE STRUCTURES COUPLED WITH A FLUID FLOW

T. FLAMENT^{1,2*}, J-F. DEÜ², A. PLACZEK¹, M. BALMASEDA¹, D-M. TRAN¹

¹ DAAA, ONERA, Université Paris Saclay F-92322 Châtillon - France,
{theo.flament,antoine.placzek,mikel.balmaseda}@onera.fr, <https://www.onera.fr/en>

² LMSSC, CNAM, 292 rue Saint-Martin - 75141 Paris cedex 03 - France,
jean-francois.deu@cnam.fr, <https://www.lmssc.cnam.fr/en>

Key words: Computational dynamics, nonlinear model order reduction, geometric nonlinearity, fluid-structure interaction, aeroelasticity.

Abstract. This work concerns the numerical modeling of the vibrations of geometrically nonlinear structures coupled with a fluid flow. Firstly, a reduced-order model (ROM) for the geometrically nonlinear structure is proposed. Then, the aforementioned ROM is used to replace a Finite Element solver (FE) in the frame of a fluid-structure partitioned coupling on a two-dimensional example involving vortex induced vibrations.

1 Introduction

The design of future aircraft engines with fans or propellers of large dimensions leads to flexible structures. The geometric nonlinearities due to the large amplitudes of displacements significantly alter the level of vibrations and a nonlinear model of the structure is therefore necessary to characterize aeroelastic phenomena such as flutter and forced response. A common approach to carry out aeroelastic simulations is to couple two separate solvers for the fluid and for the structure. The associated difficulties are the excessive computational time for industrial applications and the cumbersomeness of the coupling in terms of transfer of information from one solver to the other one. An efficient approach to overcome those problems is to couple a nonlinear fluid solver with a reduced-order model (ROM) for the structural solver, the latter being independent from the full order Finite Element Model. In our case we consider only geometric nonlinearities due to large displacements and small strain hypotheses. The ROM is built by projection on a reduced basis and the internal geometric nonlinear forces are approximated as a third order polynomial of the generalized coordinates whose coefficients are identified using the *Implicit Condensation and Expansion* (ICE) [1]. Nevertheless, for cantilever structures, this method has limited efficiency to capture the dynamics of the membrane stretching since the membrane displacement is treated as an auxiliary variable which may be post-processed with the ICE, and does not contribute to the dynamics. Our idea is to identify a relevant set of dual modes [5] during the construction of the model and to introduce it in the reduction basis in order to compute the membrane displacement instead of rebuilding it in postprocessing like the

Expansion step of the *ICE* method does. Such a ROM is coupled with the fluid solver *elsA* [3] to compute the dynamical response of a nonlinear Euler-Bernoulli beam model, placed in the wake of a fixed cylinder and subject to the unsteady forcing of a von Kármán vortex street.

2 Projection based structural reduced-order model

The structural dynamics behavior is modeled by a classical Finite Element approach, whose degrees of freedom in displacement, written \mathbf{u} , verify the dynamics equation:

$$\mathbf{M}\ddot{\mathbf{u}} + \mathbf{C}\dot{\mathbf{u}} + \mathbf{f}_{\text{int}}(\mathbf{u}) = \mathbf{f}_{\text{a}}(\mathbf{u}, \dot{\mathbf{u}})$$

where \mathbf{M} and \mathbf{C} are respectively the mass matrix and the damping matrices, while \mathbf{f}_{int} corresponds to the internal forces and \mathbf{f}_{a} are the aerodynamic follower forces associated to the aeroelastic problem.

One way to build a reduced order model is to project the equations of the dynamics on a well-chosen basis of reduced dimension \mathbf{V} . The displacements are approximated by $\mathbf{u} \approx \mathbf{V}\mathbf{q}$ where \mathbf{q} are called the generalized coordinates. In the nonlinear framework, the internal forces $\mathbf{f}_{\text{int}}(\mathbf{u})$ can be decomposed as the sum of a linear component $\mathbf{K}\mathbf{u}$ and a geometric nonlinear component $\mathbf{f}_{\text{nl}}(\mathbf{u})$, leading, after projection, to the following equation:

$$\mathbf{V}^T \mathbf{M} \mathbf{V} \ddot{\mathbf{q}} + \mathbf{V}^T \mathbf{C} \mathbf{V} \dot{\mathbf{q}} + \mathbf{V}^T \mathbf{K} \mathbf{V} \mathbf{q} + \mathbf{V}^T \mathbf{f}_{\text{nl}}(\mathbf{V}\mathbf{q}) = \mathbf{V}^T \mathbf{f}_{\text{a}} \quad (1)$$

The model is reduced because the matrix \mathbf{V} contains only a few vectors and the projected matrices have small dimensions compared to the initial problem. In the case of a coupled aeroelastic problem, the aerodynamic forces \mathbf{f}_{a} are evaluated with the fluid solver using a partitioned approach. In section 3 tests are carried out with a local arbitrary load not depending on the velocity, while aerodynamic forces are used in section 4.

2.1 Choice of the reduction basis

The linear modes of the structure $\Phi = \{\Phi_1, \dots, \Phi_n\}$ are solution of the eigenvalue equation:

$$(\mathbf{K} - \omega_i^2 \mathbf{M}) \Phi_i = \mathbf{0}$$

In the frame of linear problems, the choice of the reduction basis with the first linear modes, whose respective frequencies are included in the studied interval, is efficient to represent the dynamical behavior. On the contrary, in nonlinear cases, a coupling between some low frequency modes and high frequency modes may appear. Therefore, the choice for the reduction basis of the first linear modes is no longer efficient and the reduction basis has to be enriched in order to take into account the coupling between the modes. If the shape of the external forces to which the structure is subjected is known, static modes (nonlinear static solutions) can be interesting. The addition of static modes to the reduction basis brings information on the nonlinear behavior of the structure. Similarly, if high-fidelity nonlinear dynamic calculations have already been carried out, POD modes (Proper Orthogonal Decomposition), obtained by SVD (Singular Value Decomposition) from samples of the high-fidelity computation can be added to the reduction basis. However static modes and POD modes are very dependent on the

loading case and are therefore not adapted to cases of various loads such as those encountered in aerodynamics. Additionally, POD modes require a database of high fidelity nonlinear solutions, whose obtainment may require significant resources to perform expensive calculations. To obtain an independent nonlinear reduced-order model it is more interesting to add to the reduction basis modes containing information on the coupling between several linear modes independently from the external loading. One idea is to add modal derivatives in the reduction basis, that can be computed in several ways, with or without taking the inertia into account [8]. Their drawback is their plurality. Indeed, the number of modal derivatives drastically increases with the number of linear modes in the basis, and the more relevant modal derivatives are not known a priori. Another way to enrich the reduction basis is to use dual modes [5], computed from nonlinear static solutions obtained by imposing external loads with the shape of the first linear modes. The information contained in those nonlinear solutions, but not contained in the reduction basis (made of the first linear modes), is extracted. Then, a singular value decomposition is performed on the missing information. Finally, among the SVD solutions, the modes associated to high singular values and the modes leading to a maximal linearized strain energy are the dual modes added to the reduction basis.

2.2 Approximation of the projected nonlinear forces

During a partitioned fluid-structure coupling, a significant advantage of a *non-intrusive ROM* is that there is no need to interact with an external Finite Element (FE) solver to compute the displacement of the structure at every sub-iteration of coupling. However the ROM resulting from Eq (1) is intrusive since the evaluation of the projected nonlinear forces $\mathbf{V}^T \mathbf{f}_{nl}(\mathbf{V}\mathbf{q})$ requires back and forth exchanges between the ROM and the FEM variables. Indeed, the physical displacements $\mathbf{u} \approx \mathbf{V}\mathbf{q}$ has first to be rebuilt before the nonlinear forces $\mathbf{f}_{nl}(\mathbf{V}\mathbf{q})$ could be evaluated by the FEM solver, and finally projected to come back to the reduced space. An explicit expression of the projected nonlinear forces $\tilde{\mathbf{f}}_{nl}(\mathbf{q})$ as a function of the generalized coordinates \mathbf{q} is necessary to get a non-intrusive ROM that solves directly the structural problem in the reduced space:

$$\tilde{\mathbf{M}}\ddot{\mathbf{q}} + \tilde{\mathbf{C}}\dot{\mathbf{q}} + \tilde{\mathbf{K}}\mathbf{q} + \tilde{\mathbf{f}}_{nl}(\mathbf{q}) = \mathbf{V}^T \mathbf{f}_a$$

with $\tilde{\mathbf{M}} = \mathbf{V}^T \mathbf{M} \mathbf{V}$, $\tilde{\mathbf{C}} = \mathbf{V}^T \mathbf{C} \mathbf{V}$ and $\tilde{\mathbf{K}} = \mathbf{V}^T \mathbf{K} \mathbf{V}$ the mass, damping and stiffness matrices projected in the reduced space.

In the frame of finite displacements (small strains, large displacements and large rotations), considering a Saint-Venant Kirchhoff material, the nonlinear forces resulting from geometric nonlinearities are a third order polynomial function of the generalized coordinates. Writing $\tilde{f}_{nl}^k(\mathbf{q})$ the k^{th} coordinate of the projected nonlinear force, it can be shown that:

$$\tilde{f}_{nl}^k(\mathbf{q}) = \sum_{i=1}^{n_m} \sum_{j=i}^{n_m} \beta_{ij}^k q_i q_j + \sum_{i=1}^{n_m} \sum_{j=i}^{n_m} \sum_{m=j}^{n_m} \gamma_{ijm}^k q_i q_j q_m \quad (2)$$

with n_m the number of modes in the reduction basis, while β_{ij}^k and γ_{ijm}^k are respectively the quadratic and cubic coefficients of the polynomial of the generalized coordinates. To determine

those coefficients, two methods are found in the literature. The first one is the determination of the coefficients thanks to imposed displacements, called *STEP* [7] and its necessary corrections [2], [9]. The idea is to impose well-chosen displacements to the structure with the shape of linear combinations of the linear modes, then to compute the associated nonlinear forces with a FE solver and to identify the coefficients. The second method is a determination of the coefficients with imposed loads, called *Implicit Condensation* [6], and its *Expansion* [1]. In this case, loading cases are imposed to the structure, with load shapes following those of the linear modes. The nonlinear static solutions are computed as well as the nonlinear internal forces. From the nonlinear static solutions the generalized coordinates on the reduction basis are extracted using a least-squares method and the coefficients β_{ij}^k and γ_{ijm}^k are obtained by identification between the formula (2) and the nonlinear forces computed with the FE solver. The previously mentioned *IC* method provides an explicit expression of the projected nonlinear forces as a third order polynomial of the generalized coordinates. Moreover, the reduction basis used for the *IC* method only contains the first bending modes of the structure. This represents an advantage for more complex structures than a simple beam since for such structures the traction-compression and bending modes are not independent but coupled and therefore obtaining a relevant reduction basis becomes tedious.

3 Application to a nonlinear FE Bernoulli beam with von Kármán hypothesis per element

The following test case is a nonlinear Bernoulli beam model discretized in 50 elements in which the nonlinear von Kármán hypothesis is used, the dimensions and properties are presented in Table 1.

Beam dimensions		Material properties	
L (length)	4m	E	100GPa
h (thickness)	$7 \cdot 10^{-2}$ m	ρ	4400kg.m ⁻³
b (width)	$3h$	ν	0.3

Table 1: Dimensions and material properties of the flexible beam

Figure 1 represents the static linear and nonlinear displacements of the structure under a vertical load at the tip of 30000N. The geometric nonlinearity alters the vertical amplitude of the displacement but mostly introduces axial shortening due to the coupling between the axial and vertical displacements, as shown in the figure on the right. On the contrary, the linear computation does not lead to axial shortening, since, in the linear formulation, bending and traction-compression are not coupled. The *Implicit Condensation* method (*IC*) is tested on the previous test case (in orange in Figure 2) and its *Expansion* (*ICE*) is computed in postprocessing (in green). The reduction basis used contains the first 3 linear modes. The vertical displacement of the beam is well captured by the *IC* method, however the axial displacement is not captured since the reduction basis contains only bending modes, therefore there is no equation solving the axial displacement in the reduced system. The *Expansion* step (*ICE*) enables to perfectly rebuild the axial displacement in postprocessing.

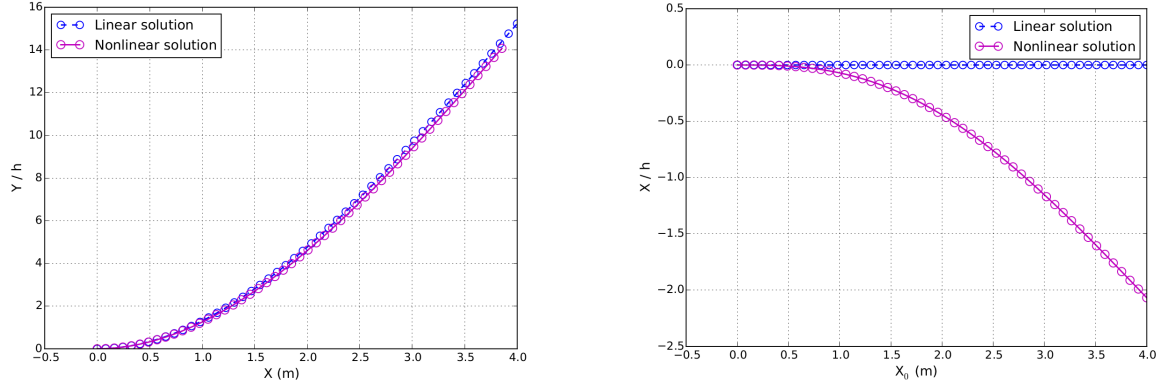


Figure 1: Nonlinear static displacement of the clamped-free Bernoulli/von Kármán beam, loaded vertically at the tip with a static load of 30000N. Comparison between the linear and the nonlinear solutions.

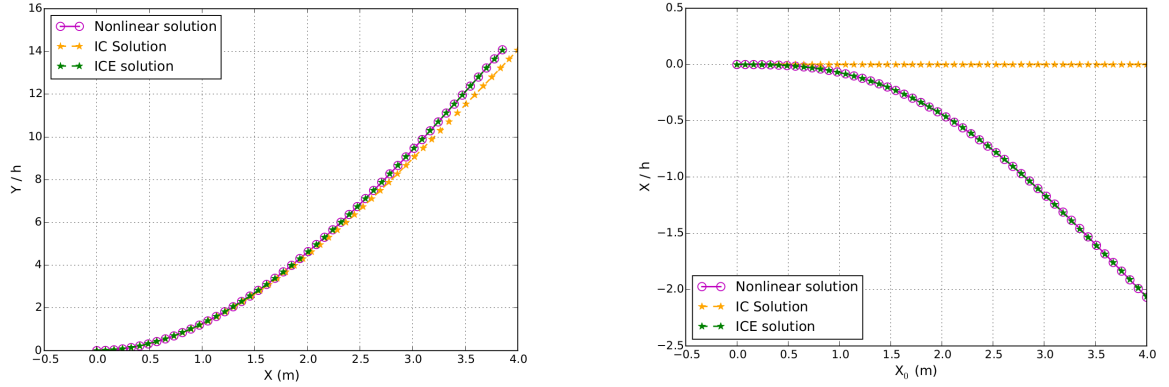


Figure 2: Static displacement (left) and axial displacement (right) of the clamped-free Bernoulli/von Kármán beam, loaded vertically at the tip with a static load of 30000N. Comparison between the nonlinear, the *IC* and the *ICE* solutions.

For the static case, the *ICE* method enabled to compute the nonlinear static solution with only 3 linear modes. Nevertheless, the solution is computed with the *IC* method and rebuilt in postprocessing with the *Expansion* step. Although good results are obtained for static cases, problems may arise for dynamic applications since the dynamics in traction-compression will not be computed with the *IC* method, leading to a significant loss of information that the bending modes will fail to capture, and that the *Expansion* step cannot rebuilt since it is based only on the generalized coordinates of the bending modes. The reduction basis should thus contain information on the nonlinear coupling between the bending and the traction-compression in order to capture the dynamics of the structure. In order to address this problem, the basis including only the first bending modes in the *Implicit Condensation* could be completed with dual modes in the reduction basis to include additional content relevant for the dynamics.

3.1 Dual modes

As previously mentioned, the reduction basis containing the first linear modes needs to be enriched in order to capture the geometric nonlinearity. The main idea of the dual modes is to add this information into the reduction basis. First a set of external forces are applied to the structure as a combination of the first linear modes $(\hat{\Phi})_{i \in [1, N]}$ of the structure:

$$\forall \ell \in [1, N_L] \quad \mathbf{f}_{\text{ext}}^{(\ell)} = \mathbf{K} \left(\sum_{i=1}^{N_L} \alpha_i^{(\ell)} \hat{\Phi}_i \right)$$

with N_L is the number of load cases and $(\alpha_i^{(\ell)})$ weighting coefficients for the amplitude.

The associated nonlinear static solution $\mathbf{u}_s^{(\ell)}$ are computed and the corresponding generalized coordinates $\mathbf{q}^{(\ell)}$ on the modes of the reduction basis are extracted by least-squares approximation since $\mathbf{u}_s^{(\ell)} \approx \hat{\Phi} \mathbf{q}^{(\ell)}$, and the residual of the approximation is written $\mathbf{r}^{(\ell)}$. For each nonlinear static solution we have $\mathbf{u}_s^{(\ell)} = \hat{\Phi} \mathbf{q}^{(\ell)} + \mathbf{r}^{(\ell)}$ and all the residuals $\mathbf{r}^{(\ell)}$ are collected in a matrix which is then approximated by a SVD. The basis $(\mathbf{d}_i)_{i \in [1, n_p]}$ (with n_p the rank of the matrix of the residuals) is the orthonormal basis that minimizes in average the distance between the residuals $\mathbf{r}^{(\ell)}$ and their orthogonal projection on the basis vectors $(\mathbf{d}_i)_{i \in [1, n_p]}$. The additional dual modes selected to add to supplement the reduction basis are the vectors $(\mathbf{d}_i)_{i \in [1, n_p]}$ with the largest singular values σ_i and those contributing the most to the linearized strain energy E_k defined as:

$$E_k = \sum_{\ell=1}^{N_L} \beta_{k\ell}^2 \mathbf{d}_k^T \mathbf{K} \mathbf{d}_k \quad \text{with} \quad \beta_{k\ell} = \frac{\mathbf{d}_k^T \mathbf{r}^{(\ell)}}{\mathbf{d}_k^T \mathbf{d}_k}$$

The reduction basis of the previous test case contains the first 3 linear modes and we want to enrich this reduction basis with dual modes. Figure 3 plots the singular values and the linearized strain energies of the dual modes candidates. The vectors $\mathbf{d}_{\{1,2,3,6,7\}}$ are the dual modes kept since they are associated to a high singular value and their linearized strain energy is significant. The new reduction basis is the concatenation of the first 3 linear modes and the 5 dual modes determined with the aforementioned criteria $\mathbf{V} = [\hat{\Phi}, \mathbf{d}_{\{1,2,3,6,7\}}]$. The coefficients of the projected nonlinear forces are then identified with the *Implicit Condensation* method by imposing a larger number of load cases still based on the first linear modes (not the dual modes).

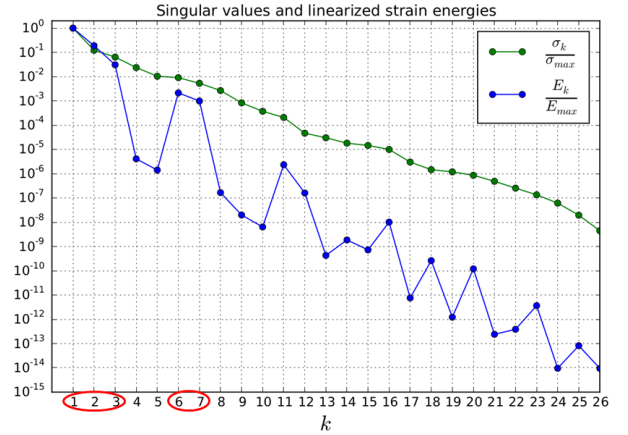


Figure 3: Singular values and linearized strain energies of the matrix of the residuals for the dual modes selection.

Since the expression of the nonlinear forces \mathbf{f}_{nl} is known analytically for our beam problem, we can identify the quadratic and cubic coefficients separately with 2 different systems. Both systems are better conditioned and better determined because the same nonlinear static solutions can be used to solve both systems. The idea of including dual modes in the reduction basis before computing the coefficients of the nonlinear forces is to avoid the *Expansion* step of the *ICE* method, by computing (instead of rebuilding in postprocessing) the coupled dynamics between the bending and the traction-compression. For the rest of the paper we will name *ICdual* the *Implicit Condensation* method with dual modes in the reduction basis, to differentiate the method from the classical *IC* method with only bending modes and from the *ICE* variant. Figure 4 represents the solution of the static test case of the previous section, this time using dual modes. The nonlinear static solution is perfectly captured with the ROM as a result of the computation, while with the *ICE* method, the same result was obtained after the *Expansion* step. This result validates the approach of enriching the reduction basis with dual modes in preprocess since the same result is obtained both with the *ICE* method and with the *ICdual* method. Nevertheless, the fact of solving the coupled dynamics of the system in bending and traction-compression (with the *ICdual* method) instead of restricting the dynamics to the bending and rebuilding the coupling afterwards (with the *ICE* method) will be of paramount importance for dynamic cases as illustrated in the following paragraph.

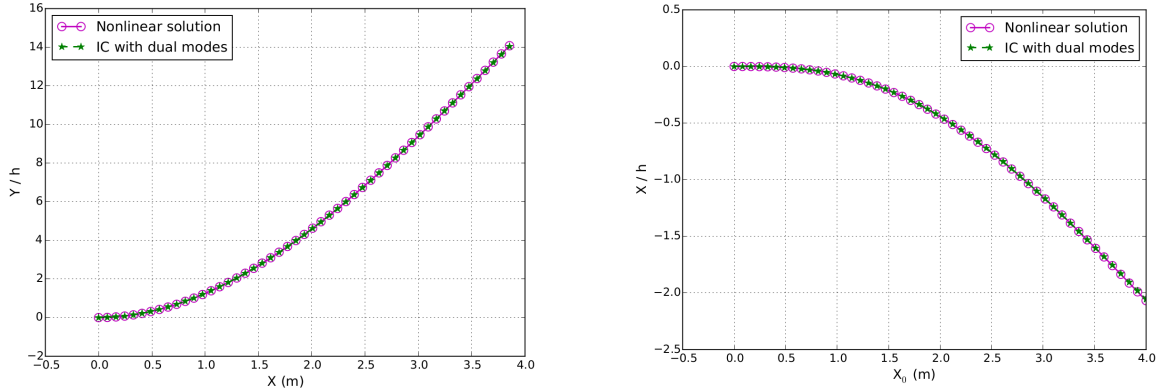


Figure 4: Static displacement (left) and axial displacement (right) of the clamped-free Bernoulli/von Kármán beam, loaded vertically at the tip with a static load of 30000N. Comparison between the nonlinear and the *IC* solution with dual modes.

3.2 Dynamic application with dual modes and comparison with *ICE*

In this section, the performance of the *ICdual* reduced-order model is analyzed in the dynamic case. The beam is still loaded vertically at the tip but with a periodic loading of amplitude 2500N and of frequency $f_0 = 3.368\text{Hz}$. Figure 5 shows the axial displacement of the tip of the beam in permanent regime. Since the vertical displacement is close between the linear and the nonlinear solutions, the main difference between the reduction methods is observed with the axial displacement. The reduced-order model using the dual modes perfectly captures the dynamics of the system, whereas the *ICE* method has a significant error. Indeed, as explained previously

on the static case, with the *ICE* method, the traction-compression dynamics of the system is not computed and therefore rebuilt with missing information. It is worth mentioning that the *Expansion* step of the *ICE* depends only on the generalized coordinates of the bending modes, not on their velocity, meaning that it depends only on the position of the beam, whatever the dynamics of it: static, quasi-static or strongly dynamic. Besides, if more bending modes are used for the *ICE* method, 8 or more, the axial solution will not be improved since the dynamics in traction-compression will still be missing in the reduced equation of the dynamics (1). However, the 5 dual modes added to the first 3 linear modes of the structure form a reduction basis containing information both on the bending and the traction-compression dynamics.

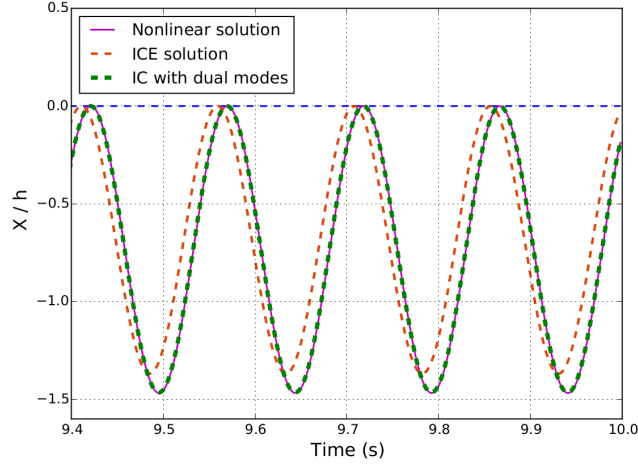


Figure 5: Nonlinear dynamic displacement of the clamped-free Bernoulli/von Kármán beam, loaded vertically at the tip with a dynamic load of amplitude 2500N and of frequency $f_0 = 3.368\text{Hz}$. The time step is $2 \times 10^{-3}\text{s}$ and the structural damping $\mathbf{C} = 2\xi\omega_0\mathbf{M}$ with $\xi = 5 \times 10^{-2}$. Comparison between the axial deformation of the nonlinear full problem, the *ICE* and the *ICdual* computations.

4 Fluid-structure interaction with a flexible beam in the wake of the cylinder

The previous application focused only the structural solver and a specific loading at one point. In this part the efficiency of the reduced-order model is investigated on a fluid-structure interaction problem. The external forces are aerodynamic forces, distributed on the beam. The aerodynamic forces result from the vortices shed in the wake of a fixed cylinder as illustrated by Figure 7 and the interaction between the flexible beam and the vortices will lead to the vibration of the beam.

The radius of the fixed cylinder is equal to $R = 1\text{m}$ and the flexible beam has the same characteristics as the one of the previous computations of this paper. The Reynolds number of the fluid flow is $Re = 200$, the density $\rho_f = 1.17\text{ kg.m}^{-3}$ and the dynamic viscosity $\mu = 0.4\text{ Pa.s}$. The mass and stiffness matrices (\mathbf{M} , \mathbf{K}) are assembled with the Bernoulli beam elements with von Kármán hypothesis per element. No structural damping is introduced in order to obtain high amplitudes of deformation. The CFD solver used is *elsA*, a finite volumes solver, and we

chose the finite volumes fluxes AUSM+ (P) MiLES since it has a low dissipation and is particularly adapted to low-Mach boundary layer flows. The time step is $dt = 4.11 \times 10^{-3}$ s. The displacements on the walls of the beam are obtained from the displacements and rotations of the middle line.

A partitioned approach is used to couple the fluid solver with the structural ROM. For each time increment, a certain number of sub-iterations between the fluid solver and the structural solver are needed in order to obtain a converged solution before moving to the next time step. Moreover those equilibrium sub-iterations can be stabilizing the coupling. The flowchart in Figure 6 summarizes the partitioned coupling between the finite volumes fluid solver *elsA* [3] and the structural nonlinear ROM. At each new time increment, a fixed-point algorithm is used between the fluid solver and the structural ROM. An ALE (Arbitrary Lagrangian Eulerian) method is used for computing the fluid dynamics in the moving mesh.

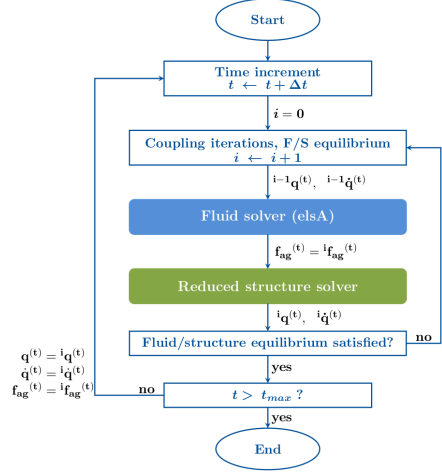


Figure 6: Flowchart of the partitioned coupling between the fluid solver *elsA* and the nonlinear reduced structural solver. We use the notation $\mathbf{f}_{ag} = \mathbf{V}^T \mathbf{f}_a$.

The structural time integration is carried out using an HHT- α method from the Newmark's family ($\alpha = 0.5$, $\beta = 0.25$) including Newton-Raphson iterations during each time steps. It is worth noting that the advantage of methods from the Newmark's family is that they are one step methods. However, the approximation of the acceleration may induce perturbations destabilizing the coupling and we were confronted to such problems. It is recommended to use HHT- α or α -generalized methods for keeping the same second-order precision but introducing a light numerical damping [4], which stabilizes the coupling. In our case we used an HHT- α integration scheme with $\alpha_{HHT} = 0.01$. The coupling depicted by Figure 6 was used to study the nonlinear coupling between a flexible beam in the von Kármán wake of a fixed cylinder, as shown in Figure 7. It is important to mention that the structural nonlinearity and the resulting large displacements represent a challenge for the temporal integration and the mesh deformation operating on a multi-block structured mesh (associated to the ALE formulation).

The integrated forces on the walls of the beam are illustrated in Figure 8 while Figure 9 represents the temporal vertical and axial displacements of the tip of the beam. Figure 10 presents respectively the vertical and axial displacements of the tip of the beam in permanent regime when the fluid-structure interaction reached a limit cycle. Observing the vertical displacement we notice a significant dephasing between the linear solution and the nonlinear solution that appeared during the transient regime. Looking at the axial displacement we witness that the linear solution has no axial displacement compared to the nonlinear solution. Both vertical and

axial displacements are well captured by the reduced-order model during the transient regime and the permanent regime. The structural solver is the reduced-order model built in the first section of this paper with the reduction basis containing the first 3 linear modes and the 5 dual modes.

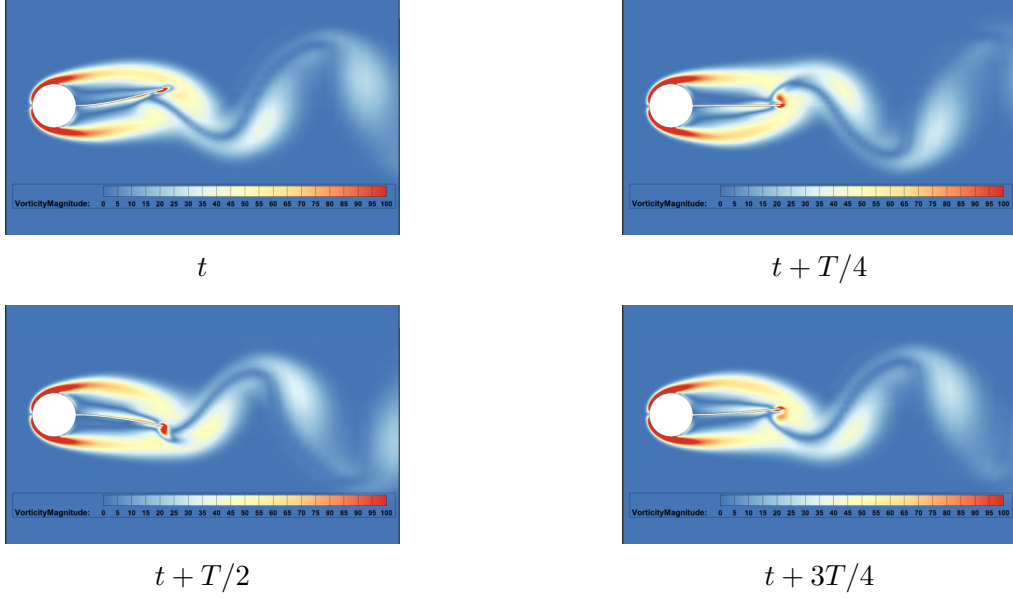


Figure 7: Fluid-structure interaction between the vortices in the wake of the cylinder and the flexible beam during one period. Visualization of the vorticity magnitude.

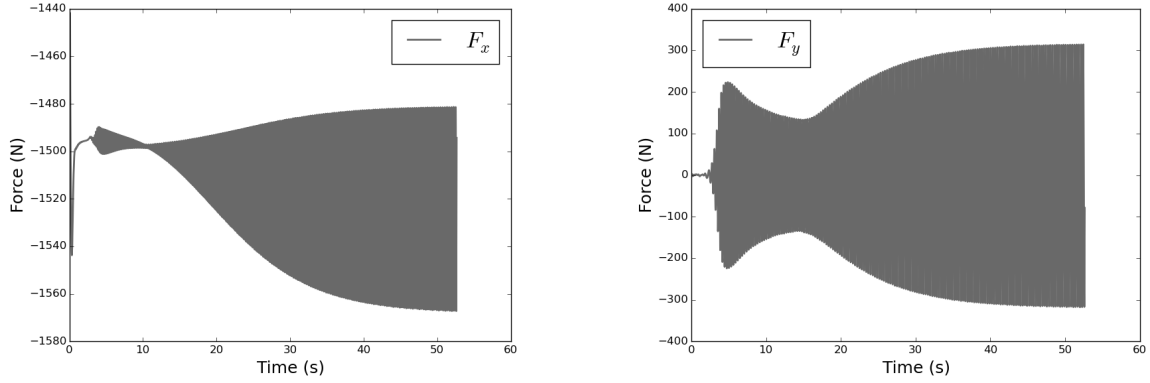


Figure 8: Time evolution of the aerodynamic forces applied to the beam. The aerodynamic forces are integrated in the surface, respectively F_x on the left and F_y on the right.

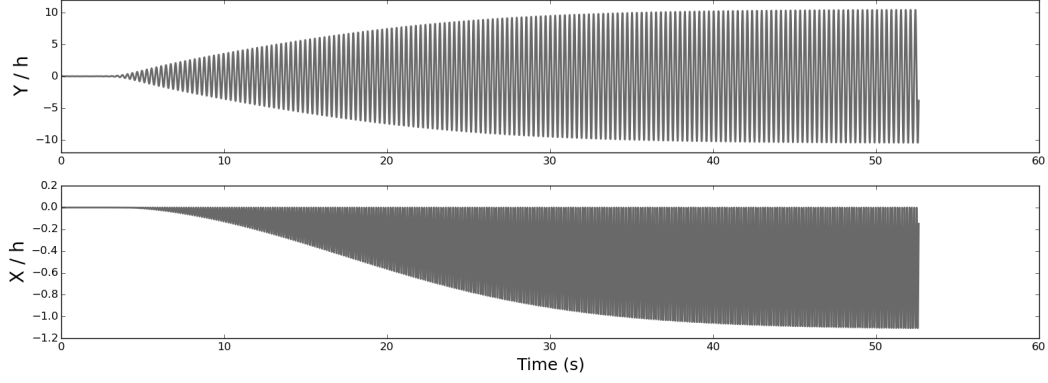


Figure 9: Vertical and axial temporal displacement of the tip of the beam.

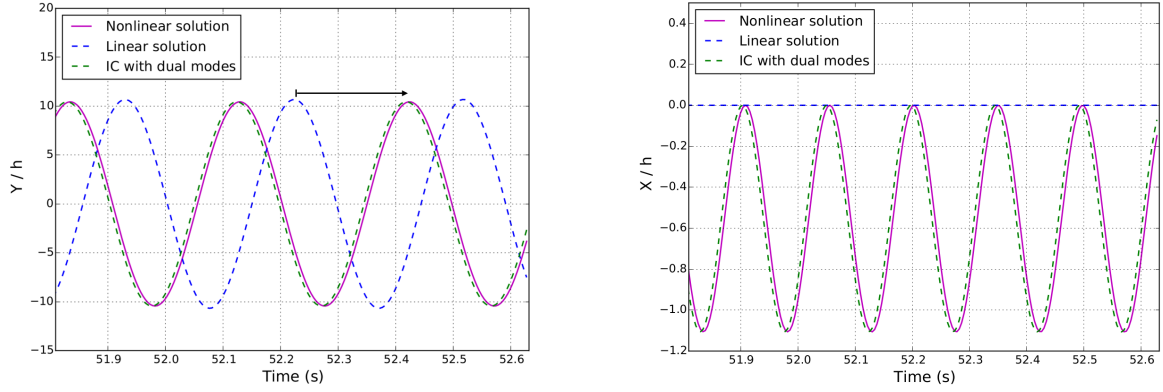


Figure 10: Vertical (left) and axial (right) displacements of the tip of the beam during the coupling in permanent regime. Comparison between the linear, the nonlinear and the reduced solutions.

5 Conclusion

In the case of geometrically nonlinear structures, reduction methods by projection on a reduction basis is not trivial due to the interaction between the linear modes of the structure. In addition to the first linear modes, dual modes are used in our case to capture the geometric nonlinearity of the structure and to better characterize the system for static and dynamic calculations. Besides, the expression of the projected nonlinear forces has to be determined as a polynomial function of the generalized coordinates in order to build a non-intrusive reduced-order model that does not need a FEM solver during the computations and therefore facilitating the coupling with the fluid solver. A partitioned approach for the coupling between the fluid solver and the structural solver was used here for flexibility reasons ie to be able to change one solver or the other more conveniently. The reduced-order model for the structural solver was built by projection on a reduced basis containing the first 3 linear modes and 5 dual modes and the projected nonlinear forces were determined explicitly as a polynomial function of the gen-

eralized coordinates whose coefficients were identified using the *Implicit Condensation* method by imposing load cases to the structure. Such a ROM showed very good results to capture the static and dynamic responses of the structure, both under local and distributed loads during a fluid-structure coupling. The perspectives in this work are the application to 3D rotating structures representative of fan or propeller blades subject to geometric nonlinearities.

Acknowledgements

This work is co-financed by the research and innovation program of the European Union Horizon 2020 in the frame of the project Clean Sky 2 ADEC and the platform LPA-IADP.

REFERENCES

- [1] J.J. Hollkamp, R.W. Gordon, Reduced-order models for nonlinear response prediction: Implicit condensation and expansion. *Journal of Sound and Vibration*, Vol. **318**, pp. 1139-1153, 2008.
- [2] M. Balmaseda, G. Jacquet-Richardet, A. Placzek, D.-M. Tran, Reduced Order Models for Nonlinear Dynamic Analysis With Application to a Fan Blade, *Journal of Engineering for Gas Turbine and Power*, Vol. **142** (4), 041002, 2020.
- [3] L. Cambier, S. Heib, S. Plot, The Onera elsA CFD software: input from research and feedback from industry, *Mechanics & Industry, EDP Sciences*, Vol. **14** (3), pp. 159-174, 2013.
- [4] M. Géradin, D.J. Rixen, Mechanical Vibrations, theory and application to structural dynamics, *John Wiley & Sons*, 2015.
- [5] K. Kim, A.G. Radu, X.Q. Wang, M.P. Mignolet, Nonlinear reduced order modeling of isotropic and functionally graded plates, *International Journal of Non-Linear Mechanics*, Vol. **49**, pp. 100–110, 2013.
- [6] M.I. McEwan, J.R. Wright, J.E. Cooper, A.Y.T. Leung, A combined modal/finite element analysis technique for the dynamic response of a non-linear beam to harmonic excitation, *Journal of Sound and Vibration*, Vol. **243** (4), pp. 601-624, 2001.
- [7] A. A. Muravyov, S. A. Rizzi, Determination of nonlinear stiffness with application to random vibration of geometrically nonlinear structures, *Computers & Structures*, Vol. **81** (15), pp. 1513-1523, 2003.
- [8] R. B. Nelson, Simplified calculation of eigenvector derivatives, *AIAA Journal*, Vol. **14** (9), pp. 1201–1205, 1976.
- [9] A. Vizzaccaro, A. Givois, P. Longobardi, Y. Shen, J.-F. Deü, L. Salles, C. Touzé, O. Thomas, Non-intrusive reduced order modelling for the dynamics of geometrically nonlinear flat structures using three-dimensional finite elements, *Computational Mechanics*, Vol. **66**, pp. 1293-1319, 2020.